

The Effect of Axial Force Variations on Nonlinear Modeling and Seismic Response of Reinforced Concrete Structures

Ebrahimi, E.¹, Abdollahzadeh, G.R.^{2*} and Jahani, E.³

¹ Ph.D. Student, Faculty of Civil Engineering, Babol Noshirvani University of Technology, Babol, Iran.

² Associate Professor, Faculty of Civil Engineering, Babol Noshirvani University of Technology, Babol, Iran.

³ Assistant Professor, Department of Civil Engineering, University of Mazandaran, Babolsar, Iran.

Received: 05 Mar. 2019;

Revised: 28 Sep. 2019;

Accepted: 13 Oct. 2019

ABSTRACT: In order to increase the accuracy of evaluating seismic response of structures, it is critical to conduct dynamic analyses based upon precise nonlinear models being as consistent as possible with the real conditions of corresponding structures. The concentrated plasticity model including one elastic element and two nonlinear spring elements at both ends has been considered within the research community for simulating beams and columns, counting the effect of strength and stiffness degradation. In this type of simulation, the axial force ratio generated in each structural component, which is a major factor in introducing nonlinear springs, has always been considered constant in the literature. The main objective of the present research is, therefore, to modify the fundamental weakness in this type of modeling approach; indeed, any variation of element's axial effort, owing to redistribution of axial forces during an earthquake, is applied in the calculation of parameters of the concentrated plasticity model as a decisive step toward the development of nonlinear dynamic analysis. Moreover, an algorithm is presented for implementing this approach in the OpenSees software. Verification is established and the efficiency of the proposed method is illustrated through a reinforced concrete moment frame subjected to a specific record, as a case study building. Regarding the results, it is confirmed that the proposed algorithm is an appropriate tool for achieving quite a realistic nonlinear model and estimating reasonably accurate responses of structural systems with cyclic degrading behavior under earthquake loading.

Keywords: Axial Load Variation, Lumped Plasticity Model, Nonlinear Dynamic Analysis, RC-Structures, Seismic Response.

INTRODUCTION

Reinforced Concrete (RC) buildings with moment-resisting frame have always been of interest to the engineering community as one

of the most widely used earthquake-resistant structural systems. However, thorough understanding of the nonlinear behavior of such buildings is not precisely possible, owing to the presence of phenomena such as

* Corresponding author E-mail: g.abdollahzadeh@ymail.com

cracking and crushing of concrete, yielding and buckling of steel bars, strain hardening, shrinkage and creep, degree of concrete confinement, and/or pinching of hysteresis loop and bond deterioration under cyclic loading. Furthermore, axial force has been proposed as one of the important factors affecting the nonlinear behavior of RC columns. Parameters such as flexural strength, stiffness, ductility and energy dissipation capacity of RC members are greatly governed by the presence of these forces or their variations (Park and Paulay, 1975).

The study of the effect of axial force variations on the behavioral characteristics of structural elements subjected to various loading conditions has always attracted the researchers' attention (Kabeyasawa et al., 1991; Razvi and Saatcioglu, 1994). In this regard, full-scale columns were tested under the influence of simultaneous lateral cyclic loading and varying compression and tensile forces, and the reports indicated a considerable effect of axial load level on the hysteretic response of columns (Saatcioglu and Ozcebe, 1989).

As for multi-story frames, the axial forces generated in columns change in the course of lateral loads like wind and earthquake. Such variations play a significant role in the flexural behavior of exterior columns of structure, especially the base-story columns, which ultimately lead to a change in the overall response of the structure against these lateral loads.

In fact, variations of axial efforts at the time of an earthquake can affect the ultimate strength, deformation capacity, and hysteretic characteristics of RC elements (Rodrigues et al., 2015). These variations can stem from the presence of vertical component of the earthquake loading or the overturning moment in the exterior columns of the lower stories of RC frames.

Xu et al. (2018) experimentally tested five

full-scale rectangular columns subjected to concurrent lateral load and varying axial load ratios, and reported that larger axial load ratios made further reduction in the lateral strength of column, ductility factor, and secondary stiffness. In order to assess the drawbacks in the previous studies, Rodrigues et al. (2013, 2015, 2018a,b) investigated the behavior of six RC columns under horizontal loading with varying axial load. They evaluated the effect of axial load variations on the failure process, stiffness and strength degradation, inelastic behavior, and energy dissipation. Based on the results, such loading pattern had a great influence on the nonlinear behavior of columns, reducing the maximum strength and yielding limit of these elements, and thus, accelerating strength degradation and reducing ductility limit. It was also observed that failure in the case of variable axial load occurred in lower drifts than those of the constant axial load case.

Saadeghvaziri et al. (1991, 1997) analytically studied the moment-curvature and the axial load-bending moment interaction curves of RC columns under variable axial loads, and showed that this loading pattern had significant impacts on the behavioral characteristic of these structural members. However, in structural level, Sadeghvaziri (1997) investigated the effects of varying axial load on the structural response based on literature and self-issued results obtained in cross-section and element level as well as the nonlinear response of bridges subjected to horizontal and vertical motions.

Ebrahimi et al. (2018) considered an 8-story RC building under earthquake records and conducted an analytical investigation into the effect of axial effort (axial force generated in structural components under seismic loading) variations in defining the behavior of nonlinear materials, determining the corresponding nonlinear model parameters, and evaluating the failure performance of the

building. For this reason, they developed a methodology utilizing the genetic algorithm and fuzzy sets theory. By considering the impact of axial effort variations, it was concluded that the probability of collapse given 2% in 50-year motion (as the structural collapse potential) and the margin against such collapse (as a simplistic indicator of collapse risk) were respectively different by 30% and 18.2% at most, as to when the axial force is considered constant.

In the context of establishing further articulation to the literature, an algorithm is presented herein to calculate the nonlinear model parameters, and to evaluate the seismic response of RC structures, considering the axial force variations of elements during the application of a specific earthquake. For this purpose, a 7-story building with an ordinary RC moment frame designed according to ACI 318-63 (1963) is selected as the case study. Thence, the lumped plasticity model proposed by Ibarra et al. (2005), being as one of the common models for simulating the behavior of RC moment frame elements (Haselton et al., 2008), is utilized for developing the nonlinear structural model. The strategy adopted in this model involves the use of an elastic element with two nonlinear spring elements at both ends to simulate each structural component. All of the linear and nonlinear parameters, required to define this model, are regression-based relationships in terms of cross-sectional and material properties of structural components recommended by Haselton et al. (2008) and implemented in OpenSEES (OpenSees, 2017).

In this paper, two-dimensional nonlinear model of the case study building is first developed based on constant axial load via OpenSees software, which is easily quantifiable under mere gravity loading conditions. It is then analyzed through incremental dynamic analysis (IDA) using the existing algorithms (Vamvatsikos and

Cornell, 2002; Asgarian et al., 2012; Haselton et al., 2016; Mohammadzadeh et al., 2018). However, after the time history analysis of building subjected to a certain record, rather than a constant axial force, an interval of axial forces is generated in each member (the length of which depends on the magnitude of earthquake, strength of utilized materials, and properties of designed sections). Subsequently, the process of nonlinear analysis is further improved using the algorithm proposed by the authors; the nonlinear model is reconstructed in each of the time history analysis step under earthquake loading, based on the axial efforts of structural elements corresponding to that step.

Investigating the characteristics of overall dynamic instability limit state (collapse point) on IDA curves, obtained from the existing and proposed algorithms, indicates that drift corresponding to collapse limit state with variable axial efforts is reduced by about 20% compared to the constant axial load condition. Since these limit states are perceived as the main inputs in establishing fragility curves and calculating the potential of structural collapse (Zareian and Krawinkler, 2007; Baker, 2015; Abdollahzadeh et al., 2015), their exact and accurate determination is therefore of great significance.

CASE STUDY BUILDING AND GROUND MOTION RECORD SELECTION

In this article, the Van Nuys Holiday Inn Hotel located in Los Angeles, California, is considered as the case study. This seven-story building with an area of 6200 m² was built in 1965, based on the ACI 318-63 code (1963), which lacks the detailing of seismic zones, e.g. the absence of shear reinforcements in the beam-to-column connection area. One of the transverse frames of the structure is selected

as illustrated in Figure 1. All geometric features and executive details are extracted from the original construction drawings provided by Rissman and Rissman Co. (Rissman, 1965). It should be noted that non-structural content vulnerability is excluded from the present study.

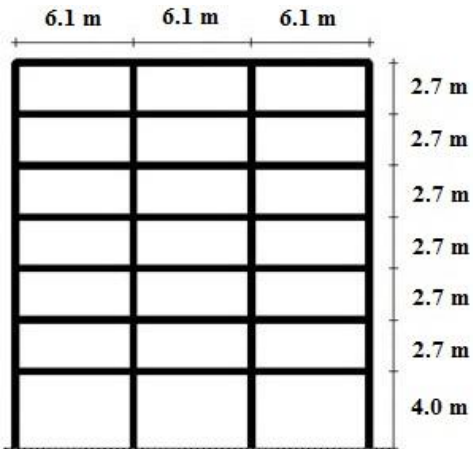


Fig. 1. The structural model used for the Van Nuys Holiday Inn frame (Vamvatsikos et al., 2003)

Then, herein, ground motion records proposed by Vamvatsikos et al. (2003) are used to select the appropriate earthquake record. They utilized a set of ground motions recorded on firm soil, bearing no marks of directivity and belonging to a bin of relatively large magnitudes of 6.5-6.9 and moderate distances. Moreover, the selected records represent the events that caused severe earthquakes on the Van Nuys site. In this paper, all the analyses are conducted under the horizontal component of the Loma Prieta earthquake, recorded in 1989 at the Waho Station (NGA-West2, 2013), as depicted in Table 1.

NONLINEAR MODELING AND DYNAMIC ANALYSIS OF THE BUILDING CONSIDERING CONSTANT AXIAL EFFORT IN STRUCTURAL COMPONENTS

Structural Component Model

The results of previous studies (Ibarra et

al., 2005; Kazantzi et al., 2014) demonstrate that hysteretic models capable of simulating the effects of strength and stiffness degradation of structural components are critical in accurate estimation of performance limit state and/or rehabilitation of a structure. In order to incorporate this type of deterioration in nonlinear modeling of the selected RC frame, all beams and columns are modeled based on the lumped plasticity concept, and using the material defined in the OpenSees software as ModIMKPeakOriented. This type of material, which is assigned to the nonlinear zero-length elements (springs) at two ends of each structural component, can simulate the peak-oriented hysteretic model developed by Ibarra, Medina, and Krawinkler, (or IMK model) (Ibarra et al., 2005). One of the most important features of this model is its ability to capture the principal modes of cyclic strength and stiffness deterioration, as well as to characterize the negative stiffness branch of post-peak response in the backbone curve, which simulates the strain-softening behavior of RC materials. The analytical model of each structural element, the backbone curve and the associated hysteretic behavior are shown in Figure 2.

Haselton et al. (2008) proposed formulas, calibrated based on 255 RC column tests, to calculate the parameters necessary for complete definition of the backbone curve and to estimate the rate of hysteretic degradation of the IMK model. In these relationships, the least number of geometric characteristics and material properties of RC members were used to estimate the required parameters. The equations utilized in this study to derive the backbone curve parameters and their corresponding descriptions are presented in Table 2.

Generic RC Moment Frame and Range of Structural Parameters Considering Constant Axial Efforts

According to the geometry of the selected moment frame of the Van Nuys building, as shown in Figure 1, the values of input parameters required by Haselton equations (as illustrated in Table 2) to estimate the backbone curve of the reinforced concrete beams and columns are respectively summarized in Tables 3 and 4. Due to rigidity of ceilings, the axial force generated in beams is negligible and thus

their axial force ratio is considered to be zero, as reported in Table 3. However, the axial force generated in columns caused by gravity loads is calculated at this stage (Haselton et al., 2008; Abad et al. 2013); indeed, assuming that structure remains elastic during gravity loads, a simple model is built using OpenSees software, regardless of the nonlinear behavior. Thence, the resulting axial forces of all columns are recorded and replaced in Table 4. The location of all beams and columns and their naming format, provided that F_i ($i = 1:7$) denotes the story number, is introduced in Figure 3a.

Table 1. Properties of selected record

No.	Event, Station, Component	Year	Mag. (Richter)	R (Km)	dt	npts	Time	PGV (m/s)	PGA (m/s ²)
1	Loma Prieta, Waho, 0.0	1989	6.9	16.9	0.005	5001	24.995	0.3812	0.654

Table 2. Introduction of model parameters and the associated equations

No	Model Parameters	Descriptions	Equations
1	M_y	Yield moment	Calculated based on Panagiotakos and Fardis (2001)
2	θ_y	Yield rotation	Calculated based on Panagiotakos and Fardis (2001)
3	EI_{eff}	Effective flexural stiffness	Calculated based on Elwood et al. (2007)
4	θ_p	Plastic rotation Capacity	$0.13(1 + 0.55a_{sl})(0.13)^v(0.02 + 40\rho_{sh})^{0.65}(0.57)^{0.01f_c}$
5	θ_{pc} (or K_c)	Post-capping rotation Capacity	$(0.76)(0.031)^v(0.02 + 40\rho_{sh})^{1.02} \leq 0.1$
6	M_c/M_y (or K_s)	Hardening stiffness ratio ($K_s = \alpha_s K_e$)	$(1.25)(0.89)^v(0.91)^{0.01f_c}$
7	λ	Normalized hysteretic energy dissipation capacity (cyclic)	$(170.7)(0.27)^v(0.1)^{s/d}$
8	c	Exponent term to model rate of deterioration (cyclic)	For constant rate of deterioration = 1.0

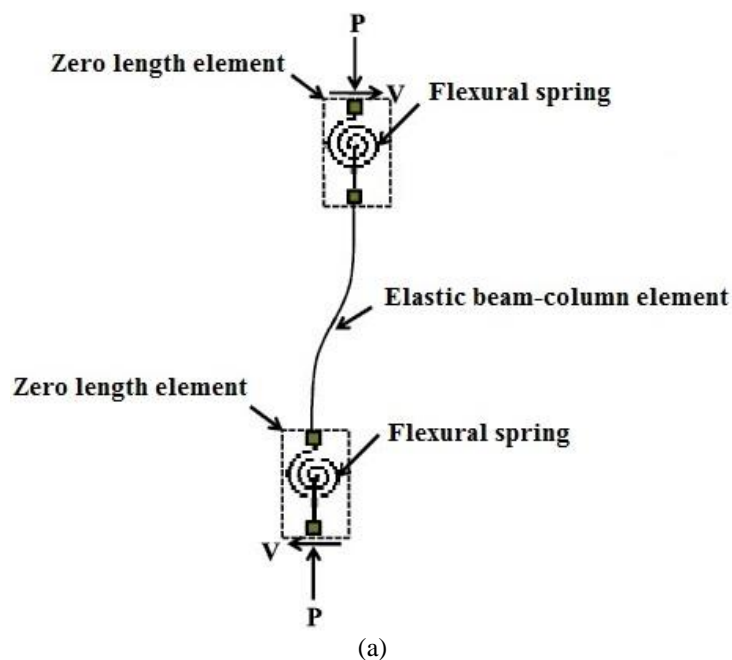
a_{sl} : is a bond-slip indicator ($a_{sl} = 1$ where bond-slip is possible), v : is the axial load ratio ($P/A_g f_c$), P : is value from gravity load calculations, A_g : is gross cross-sectional area (mm²), ρ_{sh} : is the area ratio of transverse reinforcement in the plastic hinge region spacing (A_{sh}/sB), A_{sh} : is total cross-sectional area of transverse reinforcement within spacing, s , B : is width of section, measured perpendicular to transverse load, f_c : is compressive strength of unconfined concrete based on standard cylinder test (MPa), s : is stirrup spacing measured along height of section (region of close spacing), and d : is effective depth of section ($h - \hat{d}$) (mm).

Table 3. Values of the main variables required in the Haselton equations for estimating the backbone curve parameters of beam elements

SecID	EleID	A_g (mm ²)	s (mm)	A_{sh} (mm ²)	ρ_{sh}	f'_c (MPa)	v	a_{sl}
F1SB1-F1SB2-F1SB3	232-222-212	270967.2	127	142	0.003144292	27.579	0	1
F2SB1-F2SB2-F2SB3	233-223-213							
F3SB1-F3SB2-F3SB3	234-224-214							
F4SB1-F4SB2-F4SB3	235-225-215	203225.4	127	142	0.003144292	20.684	0	1
F5SB1-F5SB2-F5SB3	236-226-216							
F6SB1-F6SB2-F6SB3	237-227-217							
F7SB1-F7SB2-F7SB3	238-228-218	198709.28	127	142	0.003144292	20.684	0	1

Table 4. Values of the main variables required in the Haselton equations for estimating the backbone curve parameters of column elements

SecID	EleID	A_g (mm ²)	s (mm)	A_{sh} (mm ²)	ρ_{sh}	f'_c (MPa)	P (N)	v	a_{sl}
F1SC1	111	180644.8	304.8	142	0.00131012	34.4738	736723	0.12	1
F1SC2	121	180644.8	304.8	284	0.00262024	34.4738	1035450	0.17	1
F1SC3	131	180644.8	304.8	284	0.00262024	34.4738	1035450	0.17	1
F1SC4	141	180644.8	304.8	142	0.00131012	34.4738	736723	0.12	1
F2SC1	112	180644.8	304.8	64	0.00059048	27.5790	619395	0.12	1
F2SC2	122	180644.8	304.8	142	0.00131012	27.5790	870759	0.17	1
F2SC3	132	180644.8	304.8	142	0.00131012	27.5790	870759	0.17	1
F2SC4	142	180644.8	304.8	64	0.00059048	27.5790	619395	0.12	1
F3SC1	113	180644.8	304.8	64	0.00059048	20.6843	515096	0.14	1
F3SC2	123	180644.8	304.8	142	0.00131012	20.6843	721510	0.19	1
F3SC3	133	180644.8	304.8	142	0.00131012	20.6843	721510	0.19	1
F3SC4	143	180644.8	304.8	64	0.00059048	20.6843	515096	0.14	1
F4SC1	114	180644.8	304.8	64	0.00059048	20.6843	410233	0.11	1
F4SC2	124	180644.8	304.8	142	0.00131012	20.6843	572824	0.15	1
F4SC3	134	180644.8	304.8	142	0.00131012	20.6843	572824	0.15	1
F4SC4	144	180644.8	304.8	64	0.00059048	20.6843	410233	0.11	1
F5SC1	115	180644.8	304.8	64	0.00059048	20.6843	304797	0.08	1
F5SC2	125	180644.8	304.8	64	0.00059048	20.6843	424711	0.11	1
F5SC3	135	180644.8	304.8	64	0.00059048	20.6843	424711	0.11	1
F5SC4	145	180644.8	304.8	64	0.00059048	20.6843	304797	0.08	1
F6SC1	116	180644.8	304.8	64	0.00059048	20.6843	198989	0.05	1
F6SC2	126	180644.8	304.8	64	0.00059048	20.6843	276971	0.07	1
F6SC3	136	180644.8	304.8	64	0.00059048	20.6843	276971	0.07	1
F6SC4	146	180644.8	304.8	64	0.00059048	20.6843	198989	0.05	1
F7SC1	117	180644.8	304.8	64	0.00059048	20.6843	92759.7	0.02	1
F7SC2	127	180644.8	304.8	64	0.00059048	20.6843	129651	0.03	1
F7SC3	137	180644.8	304.8	64	0.00059048	20.6843	129651	0.03	1
F7SC4	147	180644.8	304.8	64	0.00059048	20.6843	92759.7	0.02	1



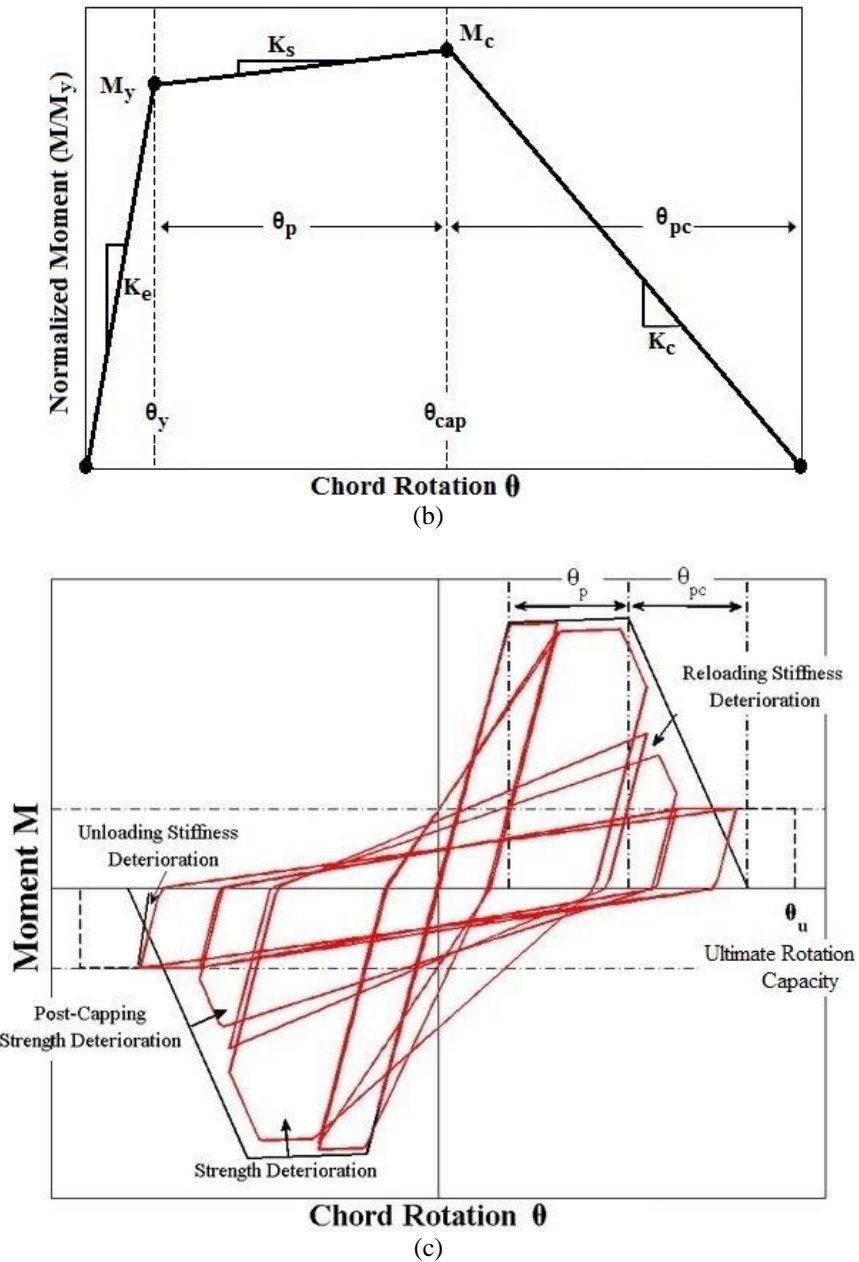


Fig. 2. Illustration of: a) the overall structure of IMK model (Gaetani d'Aragona, 2015), b) the backbone curve (Haselton et al., 2008), and c) the hysteretic behavior of IMK material model (OpenSees, 2017)

Finally, the values of parameters necessary to define the ModIMKPeakOriented materials for the rotational springs at the ends of beams and columns in the concentrated plasticity model, as shown in Figure 3b, are respectively presented in Tables 5 and 6. It is worth noting that the strain hardening ratio (α_s) is indirectly computed on the basis of relationship recommended to calculate M_c/M_y . Furthermore, the stiffness values of

the two end springs and one elastic element in between are modified, assuming that total deformation of the macro element in the plastic region is equal to the superposition of deformations of these three components connected in series (Kazantzi et al., 2014). The influence of unbalanced reinforcement is also considered for the beams, complying with the proposed relations in the reference (Panagiotakos and Fardis, 2001).

Table 5. Values of the main variables required to model the nonlinear behavior of the beam elements in OpenSees

secID	eleID	K_{mod}	$\alpha_{s,mod}$	M_y (N.m)	λ	θ_p (rad)	θ_{pc} (rad)	I_{mod} (m ⁴)
F1SB1	212	1.05E+09	0.0015012	319333.0	4.96	0.0441869	0.10	0.0043267
F1SB2	222	1.05E+09	0.0012937	266126.0	4.80	0.0427249	0.10	0.0043267
F1SB3	232	1.05E+09	0.0013378	317912.0	5.54	0.0493555	0.10	0.0043267
F2SB1	213	3.84E+08	0.0022925	166343.0	4.11	0.0427897	0.10	0.0018253
F2SB2	223	3.84E+08	0.0022925	166343.0	4.11	0.0427897	0.10	0.0018253
F2SB3	233	3.84E+08	0.0022925	166343.0	4.11	0.0427897	0.10	0.0018253
F3SB1	214	3.84E+08	0.0022925	166343.0	4.11	0.0427897	0.10	0.0018253
F3SB2	224	3.84E+08	0.0022925	166343.0	4.11	0.0427897	0.10	0.0018253
F3SB3	234	3.84E+08	0.0022925	166343.0	4.11	0.0427897	0.10	0.0018253
F4SB1	215	3.84E+08	0.0021998	165685.0	4.26	0.0444133	0.10	0.0018253
F4SB2	225	3.84E+08	0.0021998	165685.0	4.26	0.0444133	0.10	0.0018253
F4SB3	235	3.84E+08	0.0021998	165685.0	4.26	0.0444133	0.10	0.0018253
F5SB1	216	3.84E+08	0.0021998	165685.0	4.26	0.0444133	0.10	0.0018253
F5SB2	226	3.84E+08	0.0021998	165685.0	4.26	0.0444133	0.10	0.0018253
F5SB3	236	3.84E+08	0.0021998	165685.0	4.26	0.0444133	0.10	0.0018253
F6SB1	217	3.84E+08	0.0020265	167241.0	4.67	0.0486556	0.10	0.0018253
F6SB2	227	3.84E+08	0.0020735	164697.0	4.50	0.0468324	0.10	0.0018253
F6SB3	237	3.84E+08	0.0020265	167241.0	4.67	0.0486556	0.10	0.0018253
F7SB1	218	3.59E+08	0.0018406	133495.0	4.33	0.0457353	0.10	0.0017063
F7SB2	228	3.59E+08	0.0018406	133495.0	4.33	0.0457353	0.10	0.0017063
F7SB3	238	3.59E+08	0.0018406	133495.0	4.33	0.0457353	0.10	0.0017063

Table 6. Values of the main variables required to model the nonlinear behavior of the column elements in OpenSees

SecID	eleID	K_{mod}	$\alpha_{s,mod}$	M_y (N.m)	λ	θ_p (rad)	θ_{pc} (rad)	I_{mod} (m ⁴)
F1SC1	111	5.66E+08	0.0064978	447345.01	0.68	0.0236670	0.034618	0.0013675
F1SC2	121	6.54E+08	0.0059390	632801.64	0.83	0.0305740	0.051068	0.0015811
F1SC3	131	6.54E+08	0.0059390	632801.64	0.83	0.0305740	0.051068	0.0015811
F1SC4	141	5.66E+08	0.0064978	447345.01	0.68	0.0236670	0.034618	0.0013675
F2SC1	112	7.50E+08	0.0042204	275095.56	0.51	0.0174814	0.020217	0.0013675
F2SC2	122	8.67E+08	0.0047274	462894.68	0.59	0.0219246	0.028451	0.0015811
F2SC3	132	8.67E+08	0.0047274	462894.68	0.59	0.0219246	0.028451	0.0015811
F2SC4	142	7.50E+08	0.0042204	275095.56	0.51	0.0174814	0.020217	0.0013675
F3SC1	113	6.90E+08	0.0043113	253950.86	0.51	0.0176775	0.019289	0.0014529
F3SC2	123	7.92E+08	0.0049720	433227.69	0.57	0.0219550	0.026697	0.0016666
F3SC3	133	7.92E+08	0.0049720	433227.69	0.57	0.0219550	0.026697	0.0016666
F3SC4	143	6.90E+08	0.0043113	253950.86	0.51	0.0176775	0.019289	0.0014529
F4SC1	114	6.29E+08	0.0042270	235891.29	0.56	0.0187193	0.021264	0.0013247
F4SC2	124	7.10E+08	0.0044006	363214.42	0.66	0.0238118	0.030655	0.0014957
F4SC3	134	7.10E+08	0.0044006	363214.42	0.66	0.0238118	0.030655	0.0014957
F4SC4	144	6.29E+08	0.0042270	235891.29	0.56	0.0187193	0.021264	0.0013247
F5SC1	115	6.09E+08	0.0038724	217471.14	0.62	0.0198286	0.023454	0.0012820
F5SC2	125	6.29E+08	0.0042949	238399.69	0.55	0.0185719	0.020980	0.0013247
F5SC3	135	6.29E+08	0.0042949	238399.69	0.55	0.0185719	0.020980	0.0013247
F5SC4	145	6.09E+08	0.0038724	217471.14	0.62	0.0198286	0.023454	0.0012820
F6SC1	116	6.09E+08	0.0034006	198699.36	0.68	0.0210079	0.025879	0.0012820
F6SC2	126	6.09E+08	0.0037458	212563.26	0.63	0.0201321	0.024069	0.0012820
F6SC3	136	6.09E+08	0.0037458	212563.26	0.63	0.0201321	0.024069	0.0012820
F6SC4	146	6.09E+08	0.0034006	198699.36	0.68	0.0210079	0.025879	0.0012820
F7SC1	117	6.09E+08	0.0029520	179537.85	0.75	0.0222624	0.028565	0.0012820
F7SC2	127	6.09E+08	0.0031050	186229.81	0.72	0.0218185	0.027602	0.0012820
F7SC3	137	6.09E+08	0.0031050	186229.81	0.72	0.0218185	0.027602	0.0012820
F7SC4	147	6.09E+08	0.0029520	179537.85	0.75	0.0222624	0.028565	0.0012820

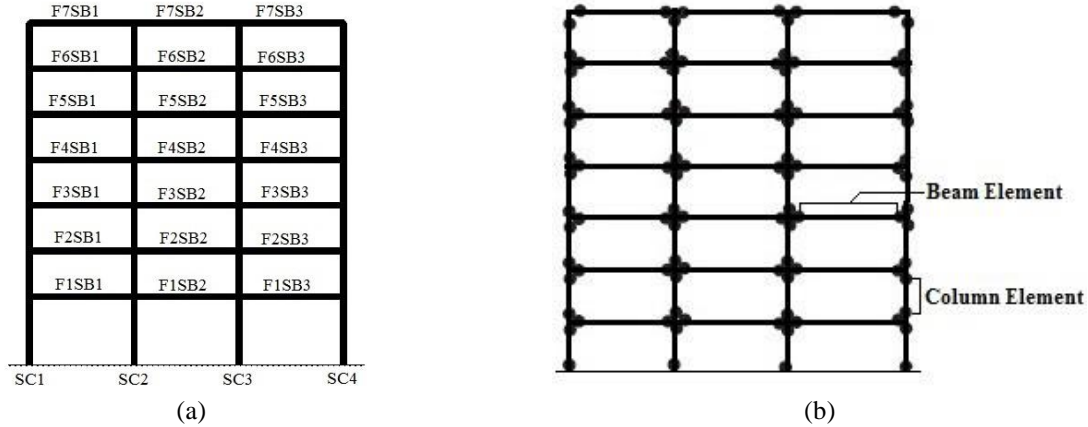


Fig. 3. Case study frame: a) the naming format for all beams and columns, b) the general form of beam and column elements in the concentrated plasticity model

Verification

The presence of an incorrect scheme in the strength degradation has significant impacts on the prediction of structural response. Thereby, in order to extract meaningful predictions from the structural analysis, the cyclic and in-cycle strength deterioration should be separated clearly and properly during the modeling process. The cyclic strength deterioration is a mode of degradation in which the strength is reduced within a loop and the element experiences a negative stiffness, so that it plays a critical role in modeling failure of the structure (Haselton et al., 2008). In the in-cycle strength deterioration, the strength decreases between the two consecutive loops, yet the stiffness remains positive. This type of

degradation is however of less importance in the structural failure modeling (Zareian and Krawinkler, 2007). In an accurate modeling process, it is then expected that the model exhibit cyclic and in-cycle strength deterioration in the small and large deformations, respectively. Accordingly, for the verification of spring elements, the formation of these degradation modes has been investigated in zero-length elements associated with column F1SC1. As depicted in Figure 4, the model experiences cyclic strength deterioration in cycles before 2% rotation and an in-cycle strength deterioration in large deformations (rotations over 2%), indicating that the values of nonlinear spring parameters have been calculated in a correct manner.

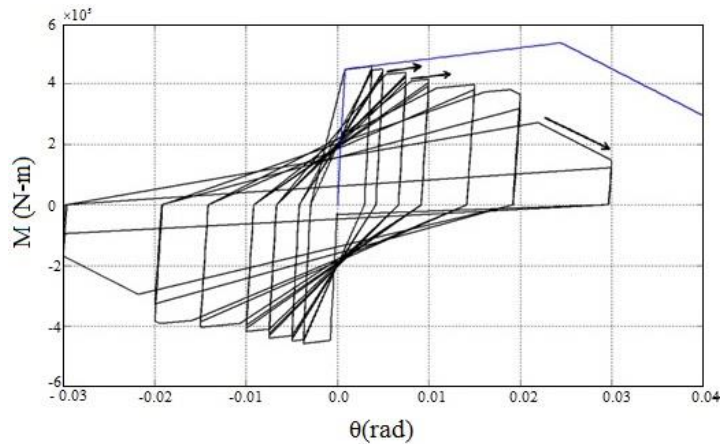


Fig. 4. Cyclic and in-cycle strength deterioration process in ModIMKPeakOriented materials of the rotational springs at two ends of column F1SC1

Incremental Dynamic Analysis (IDA)

Once the model is developed and an appropriate record is selected, IDA is utilized to analyze the structure. In this type of analysis, the selected record is scaled and applied such that the structure runs a complete path from elastic to yielding, and eventually total dynamic instability. In this paper, the Hunt & Fill algorithm, which is faster than the step algorithm and provides higher veracity of the failure point, is used to trace the IDA curve (Vamvatsikos and Cornell, 2002). In this algorithm, with increasing the intensity measure (IM) at each step, the analysis carries on until numerical divergence is reached (Hunting phase). Then, additional analyses are performed at moderate IMs, so that not only the failure point is approached, but also the level of accuracy in the lower IMs increases to an acceptable amount (Filling phase).

The most important pre-defined parameters of this algorithm are the specifying of initial step, termination rule, pattern of step increments, and the capacity and demand resolution. In this paper, the spectral acceleration at the fundamental period of the structure with 5% damping, $S_a(T_1, 5\%)$, and the maximum inter-story drift ratio, θ_{max} , are respectively taken to be as the IM (Shome and Cornell, 1999) and the demand parameters. The sequence of runs performed on different intensity measures subjected to selected ground motion is given in Table 7.

According to Table 7, the first elastic analysis is performed at 0.005 g and the algorithm terminates after 15 analyses under the selected record (Vamvatsikos and Cornell, 2002). The level of accuracy of the collapse capacity is 10%, i.e. the gap between the IM corresponding to $\theta_{max} = \infty$, and the highest converging IM is considered to be less than 10% of a preceding IM $((1.49 - 1.355) / 1.355 = 9.96\% < 10\%)$. Finally, once the dynamic analysis is performed and the

desired $S_a(T_1, 5\%)$ and θ_{max} values are extracted under the selected record, all points on the IDA curve are calculated using the appropriate interpolation method without the need for additional analysis. This algorithm is implemented in MATLAB and is capable of being linked to OpenSees.

NONLINEAR MODELING AND DYNAMIC ANALYSIS OF THE BUILDING CONSIDERING VARIABLE AXIAL EFFORT IN STRUCTURAL COMPONENTS

As discussed in previous section, all computations required to build the concentrated plasticity model are performed in terms of axial effort obtained from gravity analysis of structure's elastic model, and thus the resulting nonlinear model remains unchanged during the time history analysis. But obviously, given the nature of ground motion, the axial force generated in each component is distinct from each other at various steps of the time history analysis; and hence considering the effect of these changes in creating a model as real as possible seems necessary (Rodrigues et al., 2013, 2018a,b). Accordingly, the algorithm presented in this paper is able to re-create the nonlinear model of structural elements at each time history analysis step, in terms of the axial effort of that step, and then continue the process until the completion of IDA under selected record. Thence, the spectral acceleration and drift corresponding to collapse limit state are obtainable from the IDA curve.

The Proposed Algorithm

To account for the effect of axial force variations in the nonlinear dynamic analysis, the first step is to determine the axial force interval generated in each component of the structure under a specific record. In order to consider the most effective interval and improve the computational efficiency of the

proposed algorithm, nonlinear model of the structure is developed according to Section 3. After applying the selected record and performing the time history analysis, the axial

force intervals generated in columns of the Van Nuys building frame are determined. The lower and upper bounds of force interval of each column are shown in kN in Figure 5.

Table 7. Sequence of runs in accordance with Hunt and Fill algorithm for the selected record

No.	Calculations	S _a (T ₁ ,5%) (g)	θ _{max} (%)
1		0.005	0.0243
2	0.005+0.10	0.105	0.51
3	0.105+0.10+1×0.05	0.255	1.23
4	0.255+0.10+2×0.05	0.455	1.72
5	0.455+0.10+3×0.05	0.705	2.28
6	0.705+0.10+4×0.05	1.005	3.01
7	1.005+0.10+5×0.05	1.355	4.09
8	1.355+0.10+6×0.05	1.755	+∞
9	1.355+(1.755-1.355)/3	1.49	+∞
10	(1.005+1.355)/2	1.18	3.53
11	(1.18+1.355)/2	1.2675	3.79
12	(1.18+1.005)/2	1.0925	3.28
13	(1.005+0.705)/2	0.855	2.65
14	(0.705+0.455)/2	0.58	2.02
15	(0.455+0.225)/2	0.355	1.71

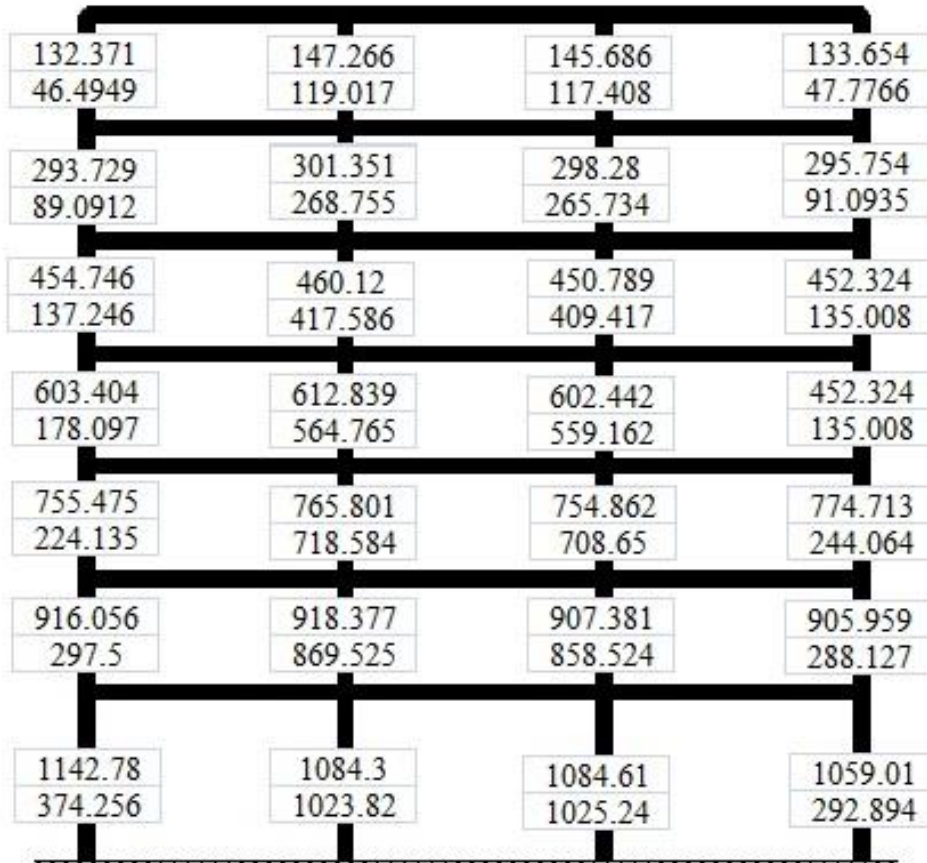


Fig. 5. The axial force interval generated in each column of selected frame under considered earthquake, kN

Regarding the numbers recorded in Figure 5, the range of axial force variations of all structural components ranges between 47.7766 kN and 1142.78 kN. In the next step, the resulting interval is partitioned into subintervals with similar coefficients of variation and the median of each one is considered as the characteristic force of the corresponding subinterval, P_{Index} . Then, the values of IMK nonlinear material parameters are calculated for each P_{Index} and classified in the form of a list in the Class.tcl file,

according to the algorithm presented in Figure 6. Thus, a reference file is created that can readily be used during analysis process. Afterwards, once the axial force generated in the structural components in each step of the time history analysis is determined, this reference file is called, so as to select the IMK parameters of the respective P_{Index} of that analysis step for each component. The proposed algorithm and the structure of the requisite OpenSees files are presented in the charts of Figures 6 and 7.

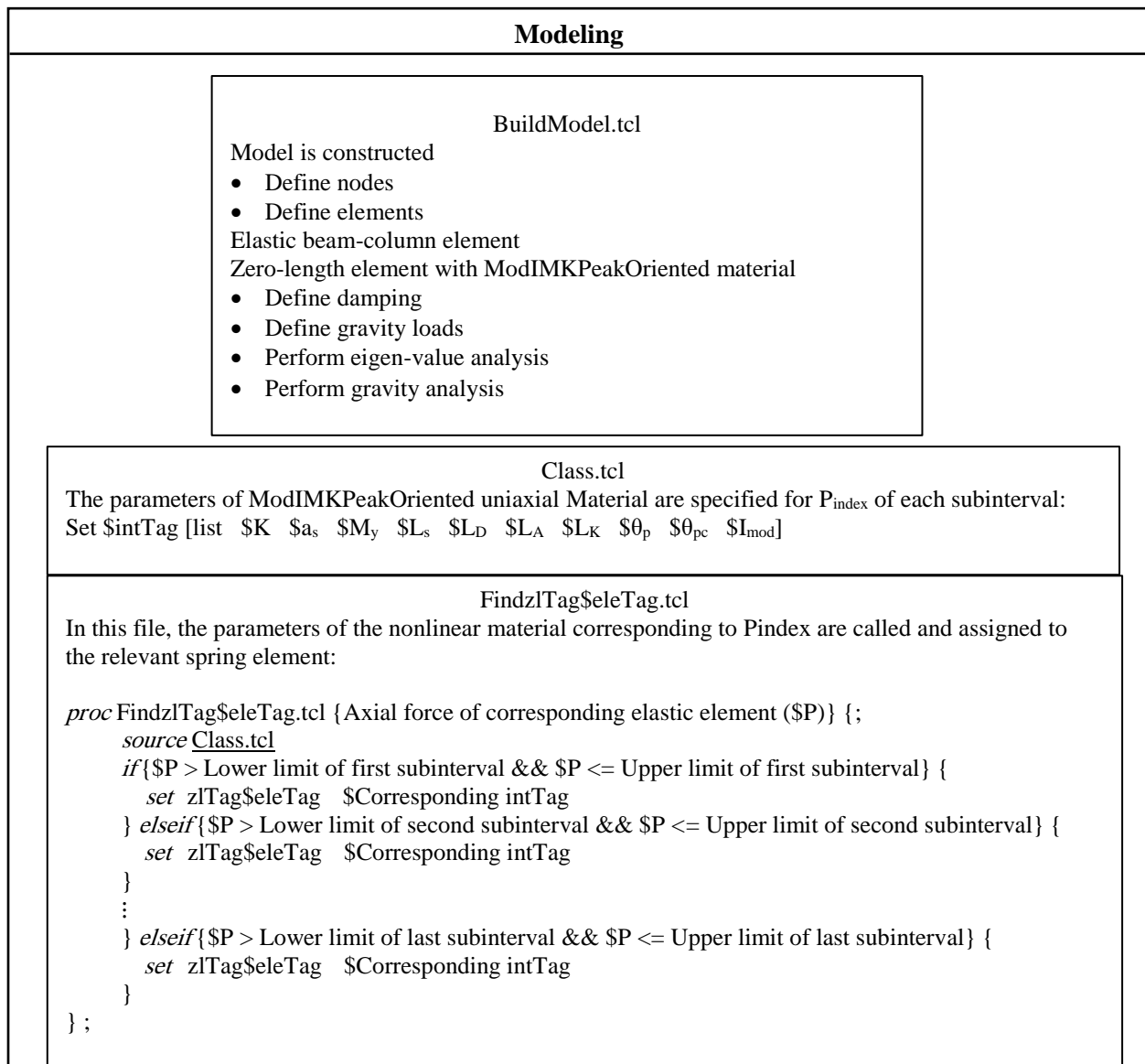


Fig. 6. The general format of files created in the OpenSees software to implement the proposed algorithm, modeling

```


Analysis



PerformIDA.tcl


Dynamic analysis with varying axial forces is performed:
  source Class.tcl
  source FindzlTag$eleTag.tcl
  The initial tags are assigned to each zero-length element of both beams and columns.
  For the selected record:


- Record time step (dt)
- Record Number of acceleration points (npts)
  - for {set i 1} {$i <= $npts} {incr i 1} {;
  - wipe
  - source BuildModel.tcl
  - Define drift recorders
  - Define element force recorder
  - Perform transient analysis {
    - If analysis is divergent or in case of an error
    - Do something to attain convergence
- Alter algorithm type
- Modify time step
  - }
  - Obtain axial force of each element from element recorder utilizing eleResponse command.

  Find ModIMKPeakOriented material parameters corresponding to calculated axial force by calling FindzlTag$eleTag.tcl procedure for each element.
  

  };

```

Fig. 7. The general format of files created in the OpenSees software to implement the proposed algorithm, analysis

In other words, in this algorithm, the nonlinear model developed based on constant axial effort (due to gravity analysis of the elastic model) is considered as the default model. Then at each step of the time history analysis, the nonlinear model developed from the new IMK parameters, which is calculated in terms of axial effort corresponding to that step of analysis, replaces the previous model and the above steps are reiterated until the termination of analysis. Finally, OpenSees file generated in the IDA structure is called in MATLAB and all the above steps are repeated at each intensity measure. The IDA curve obtained through the proposed algorithm along with one achieved from the conventional method, are depicted in Figure 8.

In order to better investigation of the results, the collapse limit states obtained from

these IDA curves are compared as a criterion for evaluating seismic response of the structure. In the case study building, values of $S_a(T_1,5\%)$ and θ_{max} , captured from the highest numerically converged run, represent the collapse limit state. Based on Figure 6 and Table 8, in addition to apparent distinction in the form of acquired IDA curves, major disparity also exists in the collapse limit states that are defined respecting these curves.

Performance Evaluation of the Proposed Algorithm

According to the results presented in Figure 8 and Table 8, when the nonlinear model of building changes during the analysis in terms of axial efforts of structural components, values of θ_{max} and $S_a(T_1,5\%)$ corresponding to collapse limit state, decrease by 20% and 14% as to when the

axial efforts are assumed constant. However, initial stiffness is not significantly affected by the axial effort variation under selected earthquake record. The reduction in the maximum inter-story drift corresponding to collapse limit state of the case study building is quite a reasonable trend. This is due to the variations of axial forces generated in columns, particularly in the corner ones, where their inelastic behavior appears to begin at smaller displacements (equations presented in Table 2), affecting the overall behavior of structure in accordance with Figure 8.

In order to control the accuracy of structural capacity variations, the moment-curvature hysteretic curves of the nonlinear rotational springs are investigated under various axial load ratios ($\nu = 0.0, 0.3, 0.7$) for column F1SC1. According to Figure 9, in the case of $\nu = 0.0$, the hysteretic cycles are rather spindle shaped, ductility and the energy dissipation capacity are acceptable conforming to the selected design codes, and the strength degradation due to cyclic loading is negligible. At $\nu = 0.3$, the strength reduces in relatively earlier cycles after reaching its maximum value, and in the case of $\nu = 0.7$, the fracture behavior is highly brittle. In fact,

an increase in the axial force ratio, according to the equations presented in Table 2, decreases the values of θ_p , M_c/M_y and θ_{pc} . However, parameters such as M_y reveal the opposite trend, so they may be increased with any increase in axial force ratio. These results are compatible with the outcomes of the proposed algorithm as depicted in Figure 8.

Indeed, Figures 8 and 9 and equations presented in Table 2 illustrate how a change in the axial load ratio may have a significant overall impact on the predicted values of nonlinear zero-length element parameters. These variations represent a change in the physical behavior of the element before and after the occurrence of phenomena such as yielding and buckling of longitudinal steel bars, cracking of concrete, crushing of concrete in the confined area, or fracture of stirrups. Consequently, modeling of nonlinear behavior based on any increase or decrease in the axial force ratio of structural components at each step of time history analysis, respectively provides a more accurate examination of the nonlinear behavior of RC members and the achievement of more realistic seismic responses.

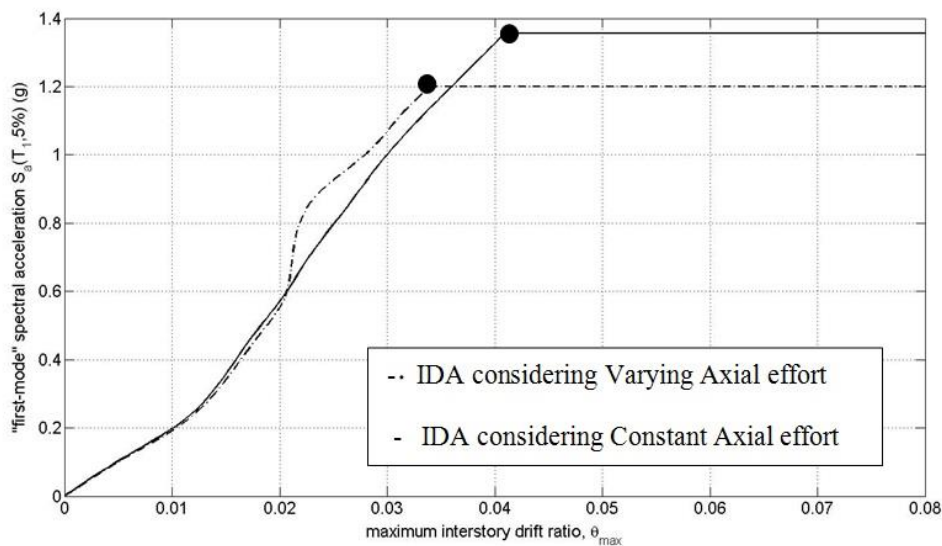


Fig. 8. Illustration of IDA curves and the collapse limit states, considering the constant and variable axial efforts during the dynamic analysis under the selected record

Table 8. Values of $S_a(T_1,5\%)$ and θ_{max} corresponding to collapse limit state for the selected record

Earthquake record	Model properties	$S_a(T_1,5\%)$ (g)	θ_{max}
Loma Prieta, Waho, 0.0	Model with Constant Axial effort	1.36	0.0418881
	Model with Varying Axial effort	1.19	0.0335336

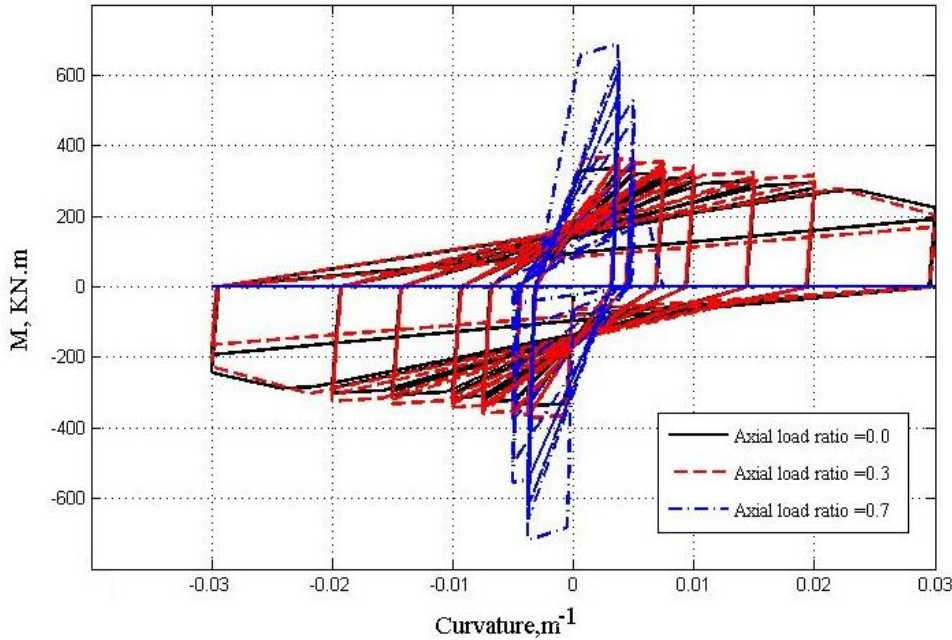


Fig. 9. The moment rotation relationship of the spring element connected with column F1SC1 with axial load ratios of 0.0, 0.3 and 0.7

CONCLUSIONS

In this research, the effect of variations in axial effort ratios of elements due to redistribution of axial forces during earthquake loading is considered in calculating the nonlinear model parameters of a structure and its dynamic analysis. An algorithm is then proposed for the nonlinear modeling of RC structures with variable axial force ratios, using the concentrated plasticity concept. Findings reveal the significant impact of variations of this ratio on the nonlinear behavior of materials, column capacity, nonlinear characteristics of structure, as well as the results obtained via IDA. Regarding such variations in the modeling and nonlinear behavior of components, proportional to axial efforts generated in each step of the time history analysis, leads to: 1) considering the slightest setback of RC members in the nonlinear

region; 2) reducing capacity and demand associated with the collapse limit state of structure under selected record; and 3) obtaining as much realistic responses as possible. In the case-study building, maximum inter-story drift and spectral acceleration corresponding to fundamental period of the structure in collapse limit state are decreased, respectively, by 20% and 14%, as compared to when the axial forces are constant. These effects are especially evident in high-rises or structures with shear walls. The range of variations in axial efforts of structural components of these buildings is much larger, and thus considering the effect of such variations on defining the nonlinear properties of materials and their nonlinear dynamic analysis is rather crucial.

REFERENCES

Abad, J., Réveillère, A., Ulrich, T., Gehl, P. and

- Bernard, R. (2013). "Fragility of pre-damaged elements: Realisation of fragility functions of elements pre-damaged by other past events and demonstration on a scenario", *Deliverable 4.2-MATRIX - New methodologies for multi-hazard and multi-risk assessment methods for Europe*.
- Abdollahzadeh, G., Sajjini, M. and Asghari, A. (2015). "Seismic fragility Assessment of Special Truss Moment Frames (STMF) using the capacity spectrum method", *Civil Engineering Infrastructures Journal*, 48(1), 1-8.
- ACI 318-63. (1963). *Building code requirements for reinforced concrete*, American Concrete Institute, Detroit, MI.
- Asgarian, B., Khazaei, H. and Mirtaheeri, M. (2012). "Performance evaluation of different types of steel moment resisting frames subjected to strong ground motion through incremental dynamic analysis", *International Journal of Steel Structures*, 12(3), 363-379.
- Baker, J.W. (2015). "Efficient analytical fragility function fitting using dynamic structural analysis", *Earthquake Spectra*, 31(1), 579-599.
- Ebrahimi, E., Abdollahzadeh, G. and Jahani, E. (2019). "Assessment of axial load effect on nonlinear modeling and seismic response of reinforced concrete-structures based on fuzzy set theory using genetic algorithm", *Structural Concrete*, 20(2), 614-627.
- Elwood, K.J., Matamoros, A., Wallace, J.W., Lehman, D., Heintz, J., Mitchell, A., Moore, M., Valley, M., Lowes, L.N., Comartin, C. and Moehle, J.P. (2007). "Update to ASCE/SEI 41 concrete provisions", *Earthquake Spectra*, 23(3), 493-523.
- Gaetani d'Aragona, M. (2015). "Post-earthquake assessment of damaged non-ductile buildings: detailed evaluation for rational reparability decisions", Ph.D. Thesis, University of Naples Federico II.
- Haselton, C., Deierlein, G., Bono, S., Ghannoum, W., Hachem, M., Malley, J., Hooper, J., Lignos, D., Mazzoni, S., Pujol, S., Uang, C.M., Hortascu, A. and Cedillos, V. (2016). "Guidelines on nonlinear dynamic analysis for performance-based seismic design of steel and concrete moment frames", *In 2016 SEAOC Convention (No. CONF)*.
- Haselton, C.B., Liel, A.B., Taylor Lange, S. and Deierlein, G.G. (2008). *Beam-column element model calibrated for predicting flexural response leading to global collapse of RC frame buildings*, Berkeley, California: Pacific Earthquake Engineering Research Center, Report No. 2007/03.
- Ibarra, L.F., Medina, R.A. and Krawinkler, H. (2005). "Hysteretic models that incorporate strength and stiffness deterioration", *Earthquake Engineering and Structural Dynamics*, 34(12), 1489-1511.
- Kabeyasawa, T., Shen, F.H., Kuramoto, H. and Rubiano, N.R. (1991). "Experimental study on behavior of ultra-high-strength reinforced concrete columns under tri-axial forces", *Transactions of the Japan Concrete Institute*, 13, 279-286.
- Kazantzi, A.K., Vamvatsikos, D. and Lignos, D.G. (2014). "Seismic performance of a steel moment-resisting frame subject to strength and ductility uncertainty", *Engineering Structures*, 78, 69-77.
- Mohammadzadeh, M.R., Vahidi, K. and Ronagh, H.R. (2018). "Seismic reliability analysis of offshore fixed platforms using incremental dynamic analysis", *Civil Engineering Infrastructures Journal*, 51(2), 229-251.
- NGA-West2. (2013). *Peer ground motion database*, Available at: <http://ngawest2.berkeley.edu>.
- OpenSees (2017). *Open system for earthquake engineering simulation*, Pacific Earthquake Engineering Research Center, Available at: <http://opensees.berkeley.edu>.
- Panagiotakos, T.B. and Fardis, M.N. (2001). "Deformations of reinforced concrete at yielding and ultimate", *ACI Structural Journal*, 98(2), 135-147.
- Park, R. and Paulay, T. (1975). *Reinforced concrete structures*, John Wiley and Sons, New York.
- Razvi, S.R. and Saatcioglu, M. (1994). "Strength and deformability of confined high-strength concrete columns", *ACI Structural Journal*, 91(6), 678-687.
- Rissman, A. (1965). *Drawings of Holiday Inn building*, Rissman and Rissman Associated Ltd.
- Rodrigues, H., Arede, A., Varum, H. and Costa, A.G. (2013). "Experimental evaluation of rectangular concrete column behaviour under biaxial cyclic loading", *Journal of Earthquake Engineering and Structural Dynamics*, 42(2), 239-259.
- Rodrigues, H., Furtado, A. and Arêde, A. (2015). "Behaviour of rectangular reinforced-concrete columns under biaxial cyclic loading and variable axial loads", *Journal of Structural Engineering*, 142(1), 04015085.
- Rodrigues, H., Furtado, A., Arêde, A. and Varum, H. (2018a). "Influence of seismic loading on axial load variation in reinforced concrete columns", *E-GFOS*, 9(16), 37-49.
- Rodrigues, H., Furtado, A., Arêde, A., Vila-Pouca, N. and Varum, H. (2018b). "Experimental study of repaired RC columns subjected to uniaxial and biaxial horizontal loading and variable axial load with longitudinal reinforcement welded steel bars solutions", *Engineering Structures*, 155, 371-386.
- Saadeghvaziri, M.A. and Foutch, D.A. (1991). "Dynamic behavior of R/C highway bridges under the combined effect of vertical and horizontal earthquake motions", *Journal of Earthquake Engineering and Structural Dynamics*, 20(6), 535-

549.

- Saadeghvaziri, M.A. (1997). “Nonlinear response and modelling of RC columns subjected to varying axial load”, *Engineering Structures*, 19(6), 417-424.
- Saatcioglu, M. and Ozcebe, G. (1989). “Response of reinforced concrete columns to simulated seismic loading”, *ACI Structural Journal*, 86(1), 3-12.
- Shome, N. and Cornell, C.A. (1999). *Probabilistic seismic demand analysis of nonlinear structures*, Stanford, California: Stanford University, Report No. RMS-35.
- Vamvatsikos, D. and Cornell, C.A. (2002). “Incremental dynamic analysis”, *Earthquake Engineering and Structural Dynamics*, 31(3), 491-514.
- Vamvatsikos, D., Jalayer, F. and Cornell, C.A. (2003). “Application of incremental dynamic analysis to RC-structures”, *The FIB Symposium on Concrete Structures in Seismic Regions*, Athens, 1-12.
- Xu, G., Wu, B., Jia, D., Xu, X. and Yang, G. (2018). “Quasi-static tests of RC columns under variable axial forces and rotations”, *Engineering Structures*, 162, 60-71.
- Zareian, F. and Krawinkler, H. (2007). “Assessment of probability of collapse and design for collapse safety”, *Earthquake Engineering and Structural Dynamics*, 36, 1901-1914.